Quest: Journal of Geometry, Mathematical and Quantum Physics
e-ISSN: 3064-7282 Vol.2 Issue 6|2025

Using Density Functional Theory to Calculate Stopping Power of Lithium Ion in Some Human Body Tissues

Wejdan A. Jasim
Republic of Iraq, Ministry of Education, Najaf Directorate of Education

Abstract: Stopping power, penetration depth, and transit time of lithium ions (Li + 3) in tissues of human skull bone, jaw muscle and lung air cavity were studied. The density functional theory with modified Bethe equation was used to calculate across the energy range of 0.01 to 1000 MeV. In order to back the theoretical findings, the simulation data of lithium ions concerning the same tissues were taken via SRIM-2013 and analyzed in the MATLAB-2021. Moreover, the average ionization potentials of the tissues under test were determined, with the help of Gaussian 09W. The results of the calculated stopping power, range, and stopping time were in good agreement with the results of SRIM-2013 simulation.

Keywords: Density functional theory (DFT), Stopping power, SRIM-2013, Gaussian 09W, Human body tissues, Range, Stopping time.

Introduction

The study of how charged particles lose energy and interact with matter through stopping power has been a central topic of investigation for over a century, dating back to the early 1900s [1], the study of stopping power and energy loss of charged particles in matter has been a dynamic and critical area of study that has found many applications in ion implantation, fundamental and nuclear physics, radiation damage assessment and medical radiology[2,3]. Heavy particles that are passing through matter lose most of their energy through the ionization and excitation of atoms [4]. Stopping power, which is the average energy loss per unit route length (-dE/dx), Many parameters affect it, most importantly the charge and velocity of the projectile, physical and compositional properties of the target medium. [5,6]. Initial studies resulted in the creation of an expression of stopping power in general [6], that originates two dominant processes, the interaction with the electrons of the atomic solution (electronic stopping) and the collision with the nuclei of atoms (nuclear stopping). These two contributions are normally added together to give the total stopping power [8,9]. At lower energies, though, the electronic part can frequently be dominant, and in certain instances, we can ignore the nuclear part [7,10]. Electronic stopping arises from several mechanisms, including momentum exchange between the ion and target electrons, ionization and excitation of either the ion or target atoms, electron capture by the ion, and collective effects such as polarization and plasmon excitation [9]. Precise calculation of stopping power, energy loss, range, straggling and equivalent dose rate in air, biological tissues and polymeric materials is of extreme significance in many scientific and application areas. These are radiation dosimetry, radiobiology, including cell death, mutagenic effects, chromosomal changes and DNA recombination, and applications in radiation chemistry, clinical radiotherapy, and nuclear science [11-14]. To obtain such measurements, various experimental strategies have been established such as direct measurements of the energy loss in thin films, backscattering of multilayered substrates, gamma resonance shift techniques, self-supporting foil experiments, and indirect determinations of alpha particle stopping power in air [11-16]. Further, the energy loss, stopping power, range, and straggling of light and medium ions (H, He, Li, C, O), and the effective dose of these ions have been studied in depth both theoretically and experimentally, and their dose contributions in various human organs have been systematically documented[17].

2. Theory

One of the most common equations on the estimation of average energies was suggested by Bohr [18], and it was known as the effective projectile charge, Z2*That criterion was further developed by W. Brandt and Yarlagadda [19,20], who explained in detail the Bohr abstraction principle. By this principle the target is stripped off outer-shell electrons, the velocity of which is less than the velocity uuu of the ion which is passing at it. The usefulness of this criterion is determined by whether the projectile and the target atom are symmetrical.

Here, the effective atomic number Z2*and the effective mean excitation energy (III) of the target electrons are dependent on the energy of the projectile. The corrections to Z2*are usually similar to the inner-shell corrections at higher energies. But the change of the ratio of III to Z2*does not obey a straightforward equation depending on the coefficients of III which are typically assumed independent of energy. These corrections are taken into consideration in the refined Bethe formula, which is given as [21]

$$S_e = \frac{4\pi (Z_1^*)^2 e^4 N}{mv^2} Z_2^* \ln\left(\frac{2mv^2}{I^*}\right) \qquad (1)$$

In which the actual atomic number Z* (Z stand for Z_1 and Z_2) may be calculated relation [22];

The effective atomic number Z* (where Z is either Z_1 and Z_2) can be obtained by use of the appropriate relation.

$$Z^* = 4\pi \int_{r_b}^{\infty} r^2 \rho(r)\, dr \qquad (2)$$

where r is distance from the nucleus, rb is determined from Bohr stripping criterion v≥bvFrb=bℏ32rb13 where vFr represent the velocity of the projectile's or target atom's Thomas-Fermi orbital, b is a constant of proportional about 1.26, and ρ(r) is the electronic charge density distribution in atom. The effective mean excitation energy is given by the Lindhard and Scharff hypothesis. I* as [23];

$$\ln I^* = \frac{4\pi}{Z_2^*} \int_{r_b}^{\infty} \ln\left[\gamma \hbar \omega_p(r)\right]\, r^2 \rho(r)\, dr \qquad (3)$$

where γ=2 for Z≥30, and pr is the regional plasma frequency 4πe2r/m12 Lindhard and Scharff suggested a standard.; 2mv2≥γℏpr, Currently, the Bohr stripping criterion is the one of choice.

Energy will be lost due to an accelerating beam crossing a target. This stopping power is caused by electron and nuclei scattering, with the electronic stopping power having the greatest influence in practically all energy ranges. The power loss is determined by the power., or more specifically the speed of the packet. In terms of stopping power, it is the ability to halt a specific amount of material. The stopping power of the medium is the rate of energy lost by the particle per unit travel length. The Bethe formula is a quantum mechanical derivation with relativistic results [21],

$$-\frac{dE}{dx} = \left(\frac{Z_1^* e^2}{4\pi\varepsilon_0}\right)^2 \frac{4\pi Z_2^* \rho_m N_A}{Amc^2} \left[ln\left(\frac{2mv^2}{I}\right) - ln(1-\beta^2) - \beta^2\right] \qquad (4)$$

where eZ1* effective charge, m electron mass, I mean ionization energy, NA Avogadro's number, A Mass percentage of a mass number, Z2* number atomic, m mass density, of the stopping material. $\beta = v/c$ speed of the particle relative to speed of light in vacuum.

The distance traveled by an incident particle within a target medium is known as the stopping range (R). In proton therapy, the range is often defined as the distance from the surface of the target to the point where the dose falls to 80% of the Bragg peak. It is possible to compute the range of a particle in a material using the Continuous Slowing Down Approximation (CSDA) or the Discrete Slowing Down Approximation (DSDA) [24].

$$R(E) = \int_{E}^{0} -\frac{1}{S(E)} dE \qquad (5)$$

The stopping time is defined as the time that a charged particle takes to rest in a medium and it may be found by use of the binary-number relation in [25] that can be stated as follows:

$$t(E) = \int_{E}^{0} -\frac{1}{v\,S(E)} dE \qquad (6)$$

where v is the ion velocity.

3. Results and discussion

The Bethe formula, combined with density functional theory, was applied to calculate the stopping power, penetration range, and stopping time of Li^{+3} ions in skull bone, jaw muscle, and lung air cavity tissues across an energy interval of 10^{-2} to 10^{3} MeV. The stopping power of each constituent element within the studied tissues was determined using the Bethe equation (Eq. 4), together with the elemental weight ratios provided in Table 1.

TABLE 1: Weight ratios of elements in studied human tissues.

Tissue	H	C	N	O	Na	Mg	P	S	Ca	Cl	K
Skull bone tissue	0.001	0.087	0.025	0.320	-	0.002	0.141	0.004	0.419	-	-
Jaw muscle tissue	0.007	0.093	0.029	0.852	0.002	-	0.004	0.004	-	-	0.008
Lung air chamber tissue	0.007	0.222	0.052	0.698	0.003	-	-	0.007	-	0.008	0.003

The molecular structure of the essential chemical compounds in the structures of the studied human tissues was represented using the Gaussian 09W program and the ionization potential of the studied human tissues was computed with a set of a few basis sets of 3-21G, 6-31G, 6-311G, LanL2DZ, LanL2MB, and SDD, and the results of the calculation of the mean ionization potential of the studied human tissues are provided in Table 2.

TABLE 2: Ionization potential of studied human tissues by different basis sets.

Basis set	Skull bone tissue	Jaw muscle tissue	Lung air chamber tissue
3-21G	321.61	136.90	137.82
6-31G	337.13	138.66	139.60
6-311G	323.54	138.62	139.56
LanL2DZ	68.63	131.99	129.24
LanL2MB	68.15	127.65	125.01
SDD	116.97	135.97	137.79

Figure 1 presents the calculated stopping power of skull bone tissue (a), jaw muscle tissue (b), and lung air cavity tissue (c). In both subsections, the black curve was used to represent the findings of the SRIM-2013 simulation and the blue curve was used to demonstrate the theoretical estimations using the Bethe equation with the help of density functional theory. The red curve illustrates the mathematical adjustment of the congruence between the two sets of data. For clarity, the blue and red curves were scaled by factors of 1.1 and 1.2, respectively, in order to highlight the minor differences, as the results are otherwise nearly identical.

The plots demonstrate that the stopping power of Li^{+3} ions is directly proportional to their energy, increasing with energy until reaching a maximum value. This behavior is mainly attributed to elastic collisions between the shell electrons of the ion and those of the target material. Beyond this point, the stopping power decreases with further energy increase, due to ionization and excitation processes of the target electrons. The correlation coefficient between the data provided by the SRIM-2013 and the theoretical outcomes of this research is shown in each subfigure of Figure 1 and it is evident that the level of consistency is high and the simulation has shown great agreement with theoretical predictions.

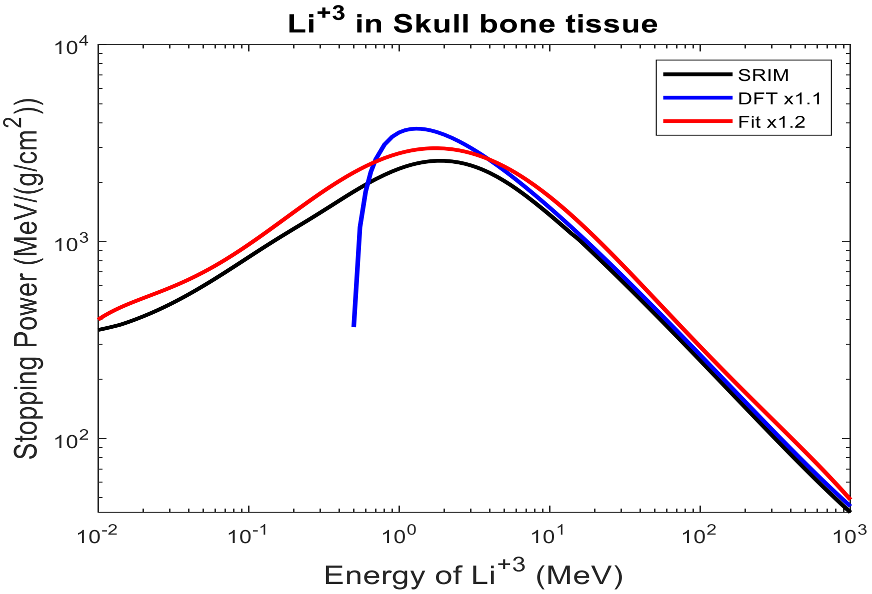

(a) $R_c = 0.9662$

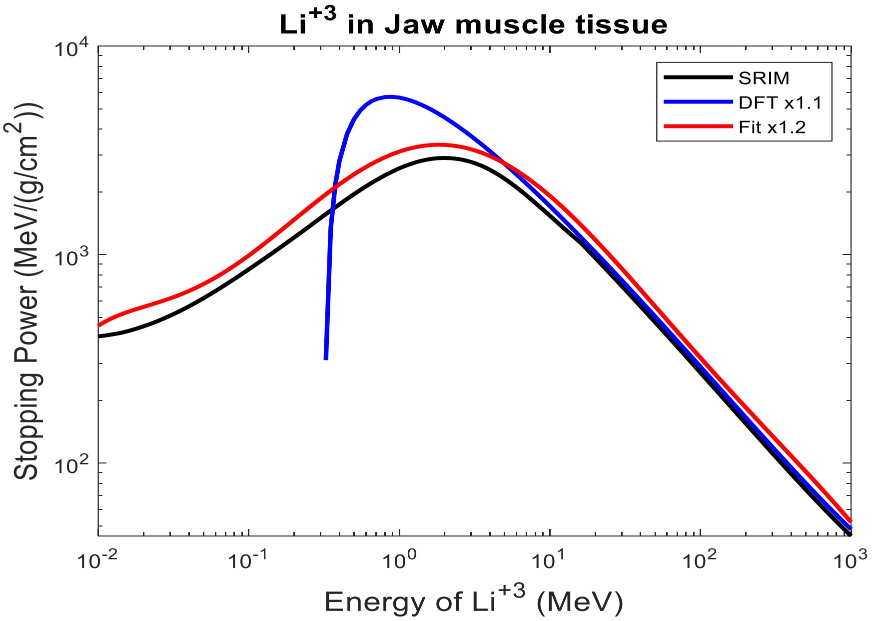

(b) $R_c = 0.9229$

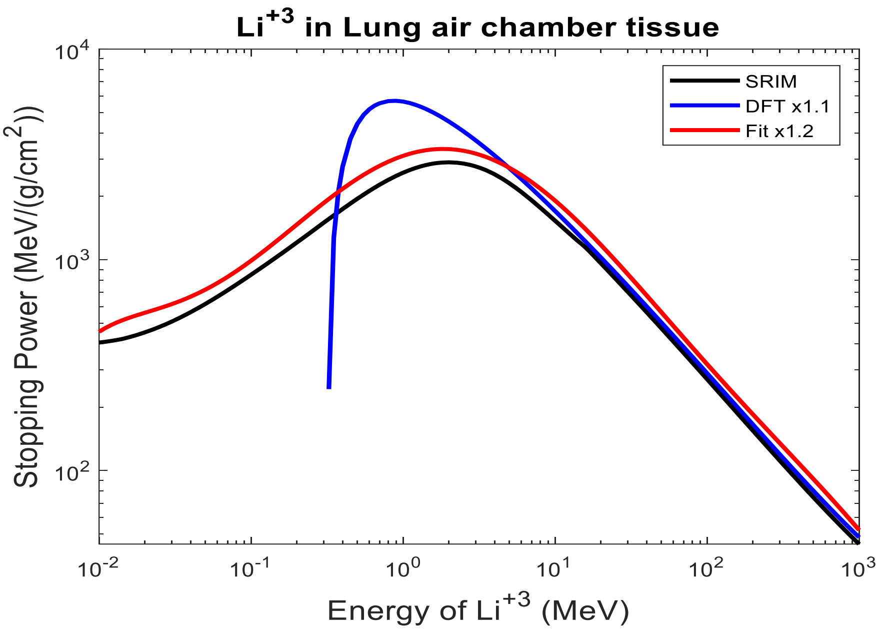

(c) $R_c = 0.9230$

FIGURE 1: Stopping power calculations for Li^{+3} ion in (a) Skull bone tissue, (b) Jaw muscle tissue, and (c) Lung air chamber tissue.

The range and stopping time of Li^{+3} ions in skull bone, jaw muscle, and lung air cavity tissues were calculated using Equations (5) and (6). The results are presented in Figures 2 and 3, with sub-sections (a), (b), and (c) corresponding to each tissue type, and plotted using the same color scheme as in Figure 1 for consistency. The stopping time exhibits a direct proportionality to the ion energy, showing an approximately linear increase as the energy rises.

At the bottom of each subfigure in Figures 2 and 3, the correlation coefficients between the SRIM-2013 simulations and the present theoretical calculations are reported. These values clearly confirm the strong agreement between the computational results obtained from SRIM-2013 and those derived in this study.

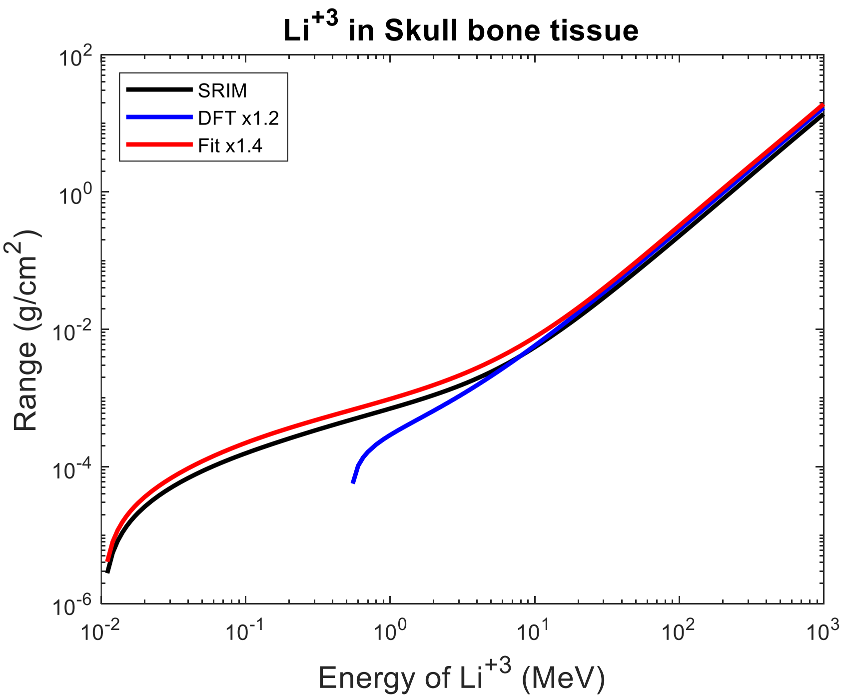

(a) $R_c = 1.0000$

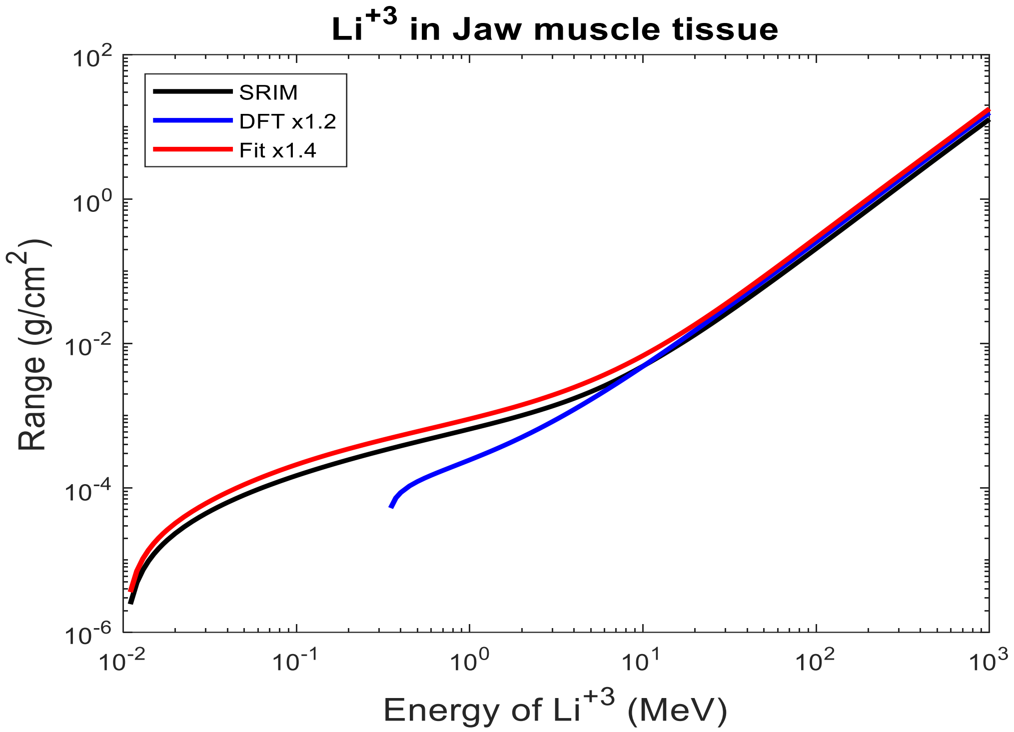

(b) R_c = 1.0000

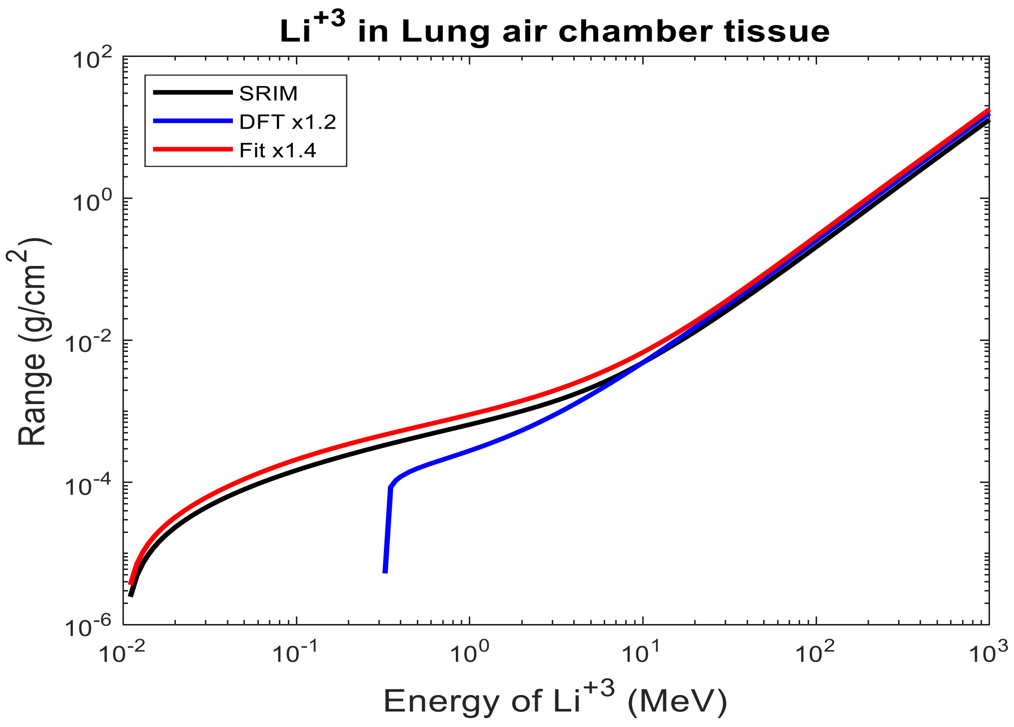

(c) R_c = 1.0000

FIGURE 2: Range calculations for Li^{+3} ion in (a) Skull bone tissue, (b) Jaw muscle tissue, and (c) Lung air chamber tissue.

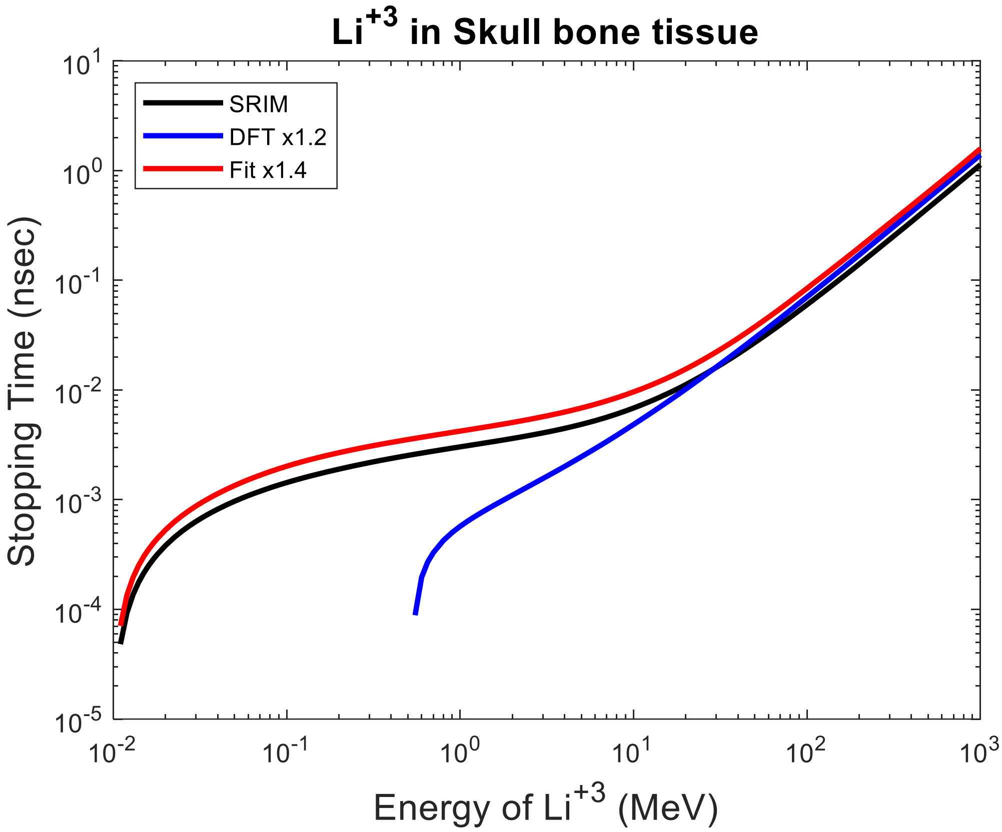

(a) R_c = 1.0000

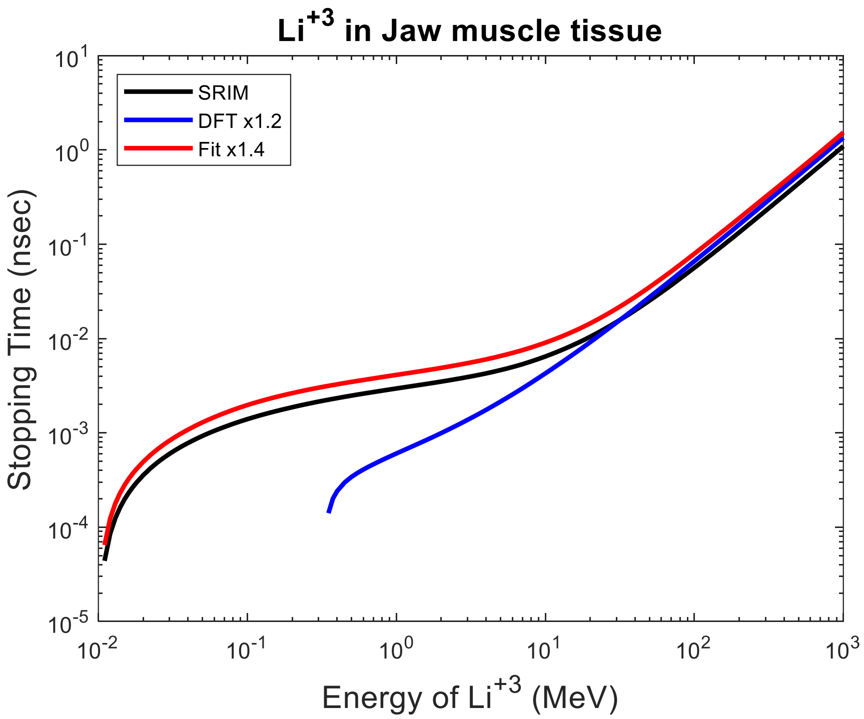

(b) R_c = 1.0000

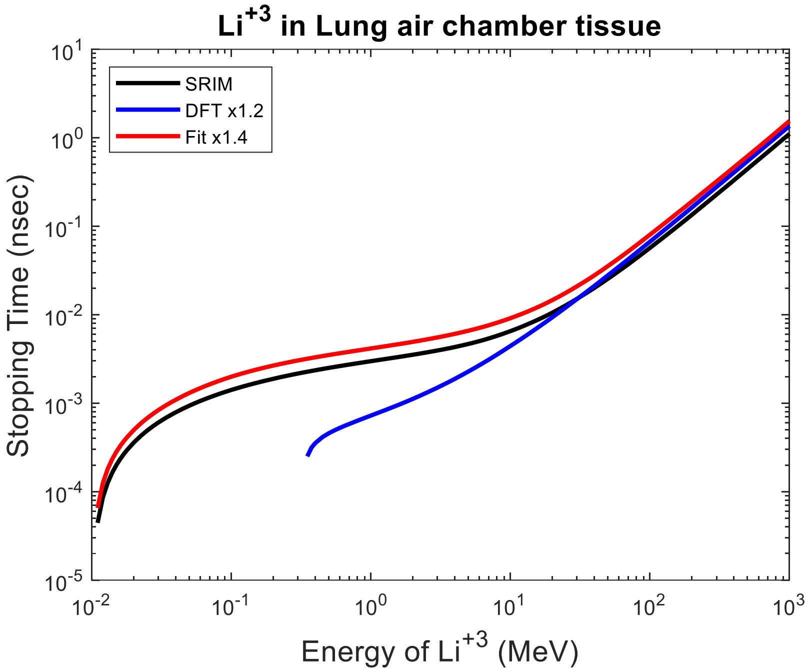

(c) R_c = 1.0000

FIGURE 3: Stopping time calculations for Li^{+3} ion in (a) Skull bone tissue, (b) Jaw muscle tissue, and (c) Lung air chamber tissue.

The correlation between the distribution of orbital electron charge density in the atomic constituents of the examined tissues, expressed in units of .ea03 and the ratio of radial distance to the Bohr radius a_0 is illustrated in Figure 4, section A. Section B illustrates how the electron charge density distribution varies as a function of the Li^{+3} ion energy. Each distribution curve begins at zero, corresponding to the atomic nucleus, and has many peaks that signify the centers of the electron shells inside each atom. The cessation of the Li^{+3} ion is minimal, but the calcium atom has twenty electrons, resulting in a substantial electronic charge density dispersion, hence significantly contributing to the attenuation of particles. Consequently, bone is the most resilient tissue against penetrating charged particles.

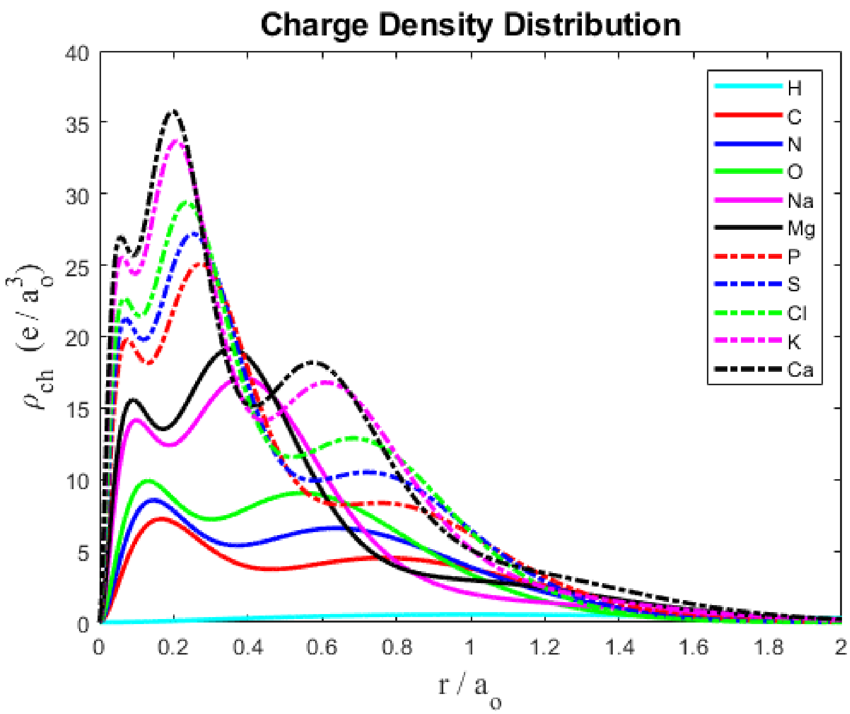

(a)

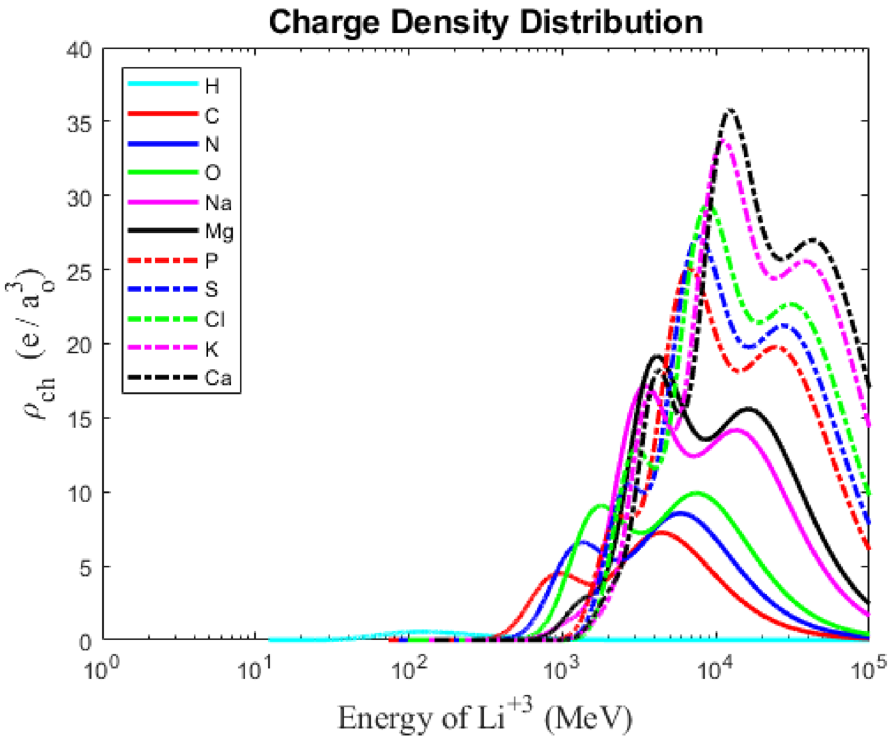

(b)

FIGURE 4: Charge density distribution of elements in studied human body tissues.

4. Conclusions

The results of this study indicate that the total stopping power, which has been calculated with the help of the Bethe equation along with the density functional theory within the energy range of 0.01-1000 MeV, increases considerably at low energies (in the range below 1 MeV). The stopping power is further increased with an increase in energy; nevertheless, the electronic contribution starts to decrease beyond 1 MeV. This is more of a trend that is determined by the velocity of the projectile as opposed to the mass of the projectile. Moreover, the curves obtained after the application of the Bethe equation to the estimation of the total stopping power in the considered tissues showed a high level of agreement with the data of the SRIM-2013 simulation, as the coefficient of correlation almost equals that value. Rc=0.9.

This research study established the efficiency of the Density Functional Theory (DFT) and the relativistic Bethe equation in determining the stopping power, range, and stopping time of lithium ion (Li^{+3}) in different tissues of the human body, which included skull bone tissue, jaw muscle tissue, and the lung air chamber tissue. The theoretical results compared well with the experimental data obtained via the SRIM-2013 software and proved the accuracy and reliability of the theoretical model employed in explaining the behavior of heavy ions in biological materials. The average ionization potential is a factor that leads to better stopping power calculations, and the fact that the Gaussian 09W software was used in obtaining more accurate estimates of this value helped. This paper has shown the significance of a combination of theoretical methods and the use of high-technology software applications including MATLAB and Gaussian to understand the interactions of particles with living tissues in more detail. This has significant medical uses including ion based radiotherapy and accurate radiation dose determination. Additionally, the methodology through which this research was conducted allows the expansion of the study to other ion or tissue types and is a potent instrument towards the development of biophysical models applied in medical and radiological computing.

References

1. J. F. Ziegler at el, (2010), SRIM – The stopping and range of ions in matter (2010), Nuclear Instruments and Methods in Physics Research B, 268, page 1818-1823.

2. Berger, M. J, ESTAR, PSTAR, ASTAR, A PC package for calculating stopping powers and ranges of electrons, protons and helium ions, Version 2, International Atomic Energy Agency, nuclear data services, documentation series of the IAEA nuclear data section, (1993).
3. National Research Council, Committee on the Biological Effects of Ionizing Radiation, Health Effects of Exposure to Low Levels of Ionizing Radiation, BEIR V, National Academy Press, Washington, D.C.,1990.
4. Fred A. Mettler, Jr., M.D. and Arthur C. Upton, M.D. Medical Effects of Ionizing Radiation, Grune & Stratton, Inc., Orlando, Florida, 1995.
5. Ahmed, S. N., physics and Engineering of Radiation Detection, Queen's University, Kingston, Ontario, (2007)118-120.
6. Y.H. Song, and Y.N. Wang, "Effect of ion-nucleus sizes on the electric stopping power for heavy ions in solids", Nucl. Instr. and Meth. in Phys. Res. B 135, 124-127, (1998).
7. W. Brandt, and M. Kitagawa, "Effective stopping-power charges of swift ions in condensed matter", Phys. Rev. B25 (9), 5631-5637, (1982).
8. L.E. Porter, "Further observations of projectile-z dependence in target parameters of modified Bethe–Bloch theory", Int. J. Quantum Chem. 95 (4-5), 504-511, (2003).
9. P.M. Echenique, R.M. Nieminen, J.C. Ashley, and R. Ritchie, "Nonlinear stopping power of an electron gas for slow ions", Phys. Rev. A33 (2), 897-904, (1986).
10. J. F. Ziegler, Nucl. Instr. Meth. B 219-220, 1027 (2004).
11. R. Macian, Biological Effects of Radiation ,Reactors Concepts Manual, USNRC Technical Training Center.
12. National Research Council, Committee on the Biological Effects of Ionizing Radiation, Health Effects of Exposure to Low Levels of Ionizing Radiation, BEIR V, National Academy Press, Washington, D.C.,1990.
13. Fred A. Mettler, Jr., M.D. and Arthur C. Upton, M.D. Medical Effects of Ionizing Radiation, Grune & Stratton, Inc., Orlando, Florida, 1995.
14. World Health Organization (.November 2012),Ionizing radiation ,health effects and protective measures.
15. A.Markowicz, Rene Van Grieken , Handbook of XRay Spectrometry, Second Edition.
16. MICHAEL F. L , ANNUNZIATA ,HANDBOOK OF RADIOACTIVITY ANALYSIS, THIRD EDITION ,2012.
17. El-Ghossain, M. O. (2017). Calculations of stopping power, and range of electrons interaction with different material and human body parts. Int J Sci Technol Res, 6(1), 114-8.
18. N. Bohr (1948). On The Notions of Causality and Complementarity, 2(3-4), 312–319.
19. W. Brandt; (1975). Atomic Collisions in Solids, Plenum Press, New York, Vol. I, p. 261.
20. B. S. Yarlagadda; J. E. Robinson; W. Brandt; (1978). Effective-charge theory and the electronic stopping power of solids. Physical Review B, 17(9), 3473–3483.
21. F. Salvat; (2022). Bethe stopping-power formula and its corrections. Physical Review A, 106(3), 032809.
22. H. Sugiyama; (1981). Electronic stopping power formula for intermediate energies. Radiation Effects, 56(3-4), 205–211.
23. M. C. Tufan; A. Koroglu; H. Gumus; (2005). Stopping power calculations for partially stripped projectiles in high energy region. Acta Phys. Pol. A 107(3), 459–472.

24. S. M. Kheradmand; R. Machrafi; (2020). Development of a new code for stopping power and CSDA range calculation of incident charged particles, part A: Electron and positron. Applied Radiation and Isotopes, 161, 109145.

25. J. E. Turner; (2008). Atoms, radiation, and radiation protection. John Wiley & Sons.